SPE 115669

Water-Flooding Incremental Oil Recovery Study in Middle Miocene to Paleocene Reservoirs, Deep-Water Gulf of Mexico

Bin Liu, Richard Dessenberger,SPE, Kenneth McMillen, SPE, Joseph Lach, SPE, Knowledge Reservoir LLC, Mohan Kelkar, SPE, University of Tulsa

This paper was prepared for presentation at the 2008 SPE Asia Pacific Oil & Gas Conference and Exhibition held in Perth, Australia, 20–22 October 2008.

Abstract

Many deep-water Gulf of Mexico discoveries of the past five years are older Tertiary reservoirs including Atlantis, Tahiti, Neptune, K-2, Thunder Horse, Shenzi, Great White, Trident, St Malo, Jack and Cascade. These middle Miocene to Paleocene reservoirs are characterized by high pressure and temperature, and low natural reservoir drive energy (due to compaction and cementation). In contrast, previous production experience in younger, Pleistocene through upper Miocene, reservoirs exhibit high primary oil recovery due to significant rock compressibility and aquifer influx. The requirement for water injection to supplement reservoir drive energy, improve oil rate, and maintain oil production rates is of primary consideration in development planning for the new, ultra-deep Gulf of Mexico discoveries. Unfortunately, there is limited production experience to use as guidance.

The purpose of this study is to provide a risk-based estimate of the incremental oil from water flooding for these types of reservoirs. A parametric simulation study was performed using experimental design to calculate incremental recovery from water-flooding in ultra-deep Tertiary reservoirs in the Gulf of Mexico. Experimental design matrices were generated for both primary and water flood scenarios, based on the selected uncertainty parameters. Proxy equations for both primary and water flood oil recovery were generated from the simulation results. Statistical Monte-Carlo simulation was run using the proxy equations. By comparing the simulation results for ten year production, water-flooding case yields a recovery factor about 20 per cent higher than no-injection case based on P50 estimate.

Introduction

Many deep-water Gulf of Mexico (GoM) discoveries of the past five years are in water depths greater than 4,000 feet and in older Tertiary reservoirs of middle Miocene to Paleocene age (yellow dots in Figure 1)[1]. Structural styles of these lower slope fields include compressional anticlines, turtle structures and sub-salt three-way dip closures against salt faces. Some of these reservoirs are highly compartmentalized by faulting. In this setting, rock compaction may be less important as a production drive mechanism, and aquifer support (possibly augmented by water flooding) assumes more significance. Porosity and permeability decrease is related to greater burial depth and compaction as well as temperature-related cementation. Older middle Miocene to Paleocene reservoirs in GoM are characterized by the following:

- Reservoirs are often at greater subsea depths: 20,000 to 30,000 ft
- Reservoirs often have high pressure (>15,000 psi) and temperature (>180°F)
- Turbidite deposition was in coalescing basin floor fans, i.e. sheet sands
- Seismic imaging is poor due to allochthonous over-hanging salt
- Reservoirs are consolidated, resulting in lower rock compressibility
- Increased diagenesis in sands with volcaniclastic components results in cementation and reduced compressibility
- Paleocene reservoirs often have poorer porosity (<15%) and permeability (<30 mD)
- Primary recovery factors are expected to be low due to the reservoir properties

Figure 1. Middle Miocene to Paleocene fields and discoveries in Gulf of Mexico

To estimate the potential incremental oil recovery brought by waterflooding, a probabilistic modeling study was performed using design of experiments (DOE) for the no-injection case and the waterflooding case, respectively. The design of experiments workflow is summarized below:

- Define uncertainty parameters and ranges based on observed reservoir properties
- Set up the first round DOE matrix including all uncertainty parameters
- Run the simulation cases defined in the matrix
- Perform a multiple regression to develop a linear relationship between recovery factor and uncertainty parameters (called the "proxy" equation) and identify the heavy hitters which have the most impact on the recovery factor
- Set up the second round DOE matrix including only the selected parameters (heavy hitters) and run the cases
- Generate a quadratic proxy equation based on the second round DOE cases
- Generate a probability density curve for recovery factor by running Monte-Carlo simulation on the proxy equation for both no-injection case and waterflooding case

Descriptions of the Model

1. Data Collection

This study concentrates on the lower Tertiary, i.e. late Miocene to Paleocene reservoirs which were found in Mississippi Canyon, Green Canyon, Atwater, Walker Ridge, and Alaminos Canyon protraction areas in Gulf of Mexico (GoM). The field data of the deepwater GoM lower Tertiary reservoirs were extensively searched through various public resources[1,2,3,4]. The collected data are directly from the records for the particular deepwater fields, including Mad Dog, Thunder Horse, Tahiti, Jack, Big Foot, Great White, Cascade, Chinook, St Malo, Trident, Tobago, K2, and Atlantis. Because all these fields are new discoveries, the data needed in this project are very scattered and require considerable searching effort. Fluid PVT data are only available for several middle Miocene age reservoirs. However, the initial pore pressure and petrophysical data for lower Tertiary reservoirs are reasonably available to define the range of main reservoir parameters. All collected data are summarized in Table 1.

According to the initial pore pressure, the lower Tertiary reservoirs can be separated into two groups, the low pressured reservoirs and the high pressured reservoirs, which are of similar vertical depth but of different pore pressure varying from 10,000 psi to 20,000 psi. The pore pressure for a particular reservoir is related to the structural setting of the field. The GoM is characterized by allochthonous salt structures. All the low pressure reservoirs are located at the seaward side (south of the salt overhang) and have large volume of communication to the gulf basin or aquifers. The high pressure fields are located at the inboard (north) of the salt margin and confined by salt or faults. Higher pressure gradients in excess of 0.75 psi/ft are often observed in the more confined reservoir settings.

PVT data is not readily available in the public domain. However, the collected data provide sufficient information to define the range of reservoir properties and to build the base model for this study.

Table 1. Collected reservoir data for lower Tertiary reservoirs in GoM

Field	YEAR OF DISCOVERY	RSI	PI	BOI	TVDSS	WATER DEPTH	THICKNESS	DRIVING MECHANISM	POROSITY	SWI	PERM	API	SPGR	kv/kh	Source
		scf/stb	psi	rb/stb	ft	ft	ft				md				
Mad Dog	2000	0	9,570	0.00	17500	4738	45.00	PAR	0.28	0.22	378.59	0	0.60		MMS.GOV
	2000	800	10,061	1.32	18400	4738	156.71	PAR	0.25	0.27	139.92	32	0.00		
	1998	280	12,397	1.15	20707	4738	170.20	WTR	0.25	0.17	456.26	30	0.00		
Thunder Horse	1999	1,458	13,684	1.25	20372	6074	32.90	DEP	0.29	0.26	320.08	34	0.00		MMS.GOV
	1999	750	15,857	1.32	22250	6074	158.53	PAR	0.26	0.16	617.17	34	0.00		
	1999	550	17,032	1.14	23900	6074	61.36	PAR	0.24	0.45	24.29	33	0.00		
	2000	1,458	15,181	1.25	21300	6074	26.48	DEP	0.24	0.20	260.11	33	0.00		
	2000	1,458	15,359	1.25	21550	6074	32.63	DEP	0.21	0.25	85.77	34	0.00		
	1999	488	17,459	1.21	24500	6074	43.92	PAR	0.23	0.26	111.08	33	0.00		
	2000	440	17,566	1.21	24650	6074	48.17	PAR	0.23	0.22	172.37	33	0.00		
	2000	488	17,512	1.21	24575	6074	47.40	PAR	0.24	0.20	260.11	33	0.00		
Tahiti	2002		20000		24000	4000	75.00	PAR	0.12			28		0.1	SPE102968: Tahiti: Assessment of Uncertainty in a Deepwater...
					27000		400.00		0.17			32		0.75	
Jack	2004				28175	7000	350.00				10 to 30				http://www.aapg.org/explorer/2006/11nov/jack_play.cfm
Big Foot					25127	5000									http://www.chevron.com/news/press/2006/2006-01-04.asp
Great White	2002		19300		15000	8000									www.worldoil.com/magazine/magazine_contents.asp
Cascade	2002				27929	8140	1150(Gross)								www.worldoil.com/magazine/magazine_contents.asp
Chinook	2003				27652	8835									www.worldoil.com/magazine/magazine_contents.asp
St Malo	2003				29066										www.worldoil.com/magazine/magazine_contents.asp
Trident	2001		10000		20500	9687	300								www.worldoil.com/magazine/magazine_contents.asp
Tobago	2004					9800									www.worldoil.com/magazine/magazine_contents.asp
K2			18700												www.worldoil.com/magazine/magazine_contents.asp
Atlantis			11400												www.aapg.org/explorer/2006/11nov/jack_play.cfm
Keathley Canyon						10000			0.18		10 to 30				www.aapg.org/explorer/2006/12nov/jack_play.cfm
Lower Tertiary GoM			20000						0.096 to 0.19		0.1 to 8.6	40			http://aapg.confex.com/aapg/2007am/techprogram/A109818.htm

2. Simulation Model

Based on the collected reservoir data, a simulation model was built to reflect the characteristics of the deepwater Gulf of Mexico reservoirs.

Geocellular and dynamic simulation models were constructed based on the stratigraphy and reservoir properties from a thick-bedded middle Miocene reservoir (e.g. Tahiti Field) and a thinner-bedded Paleocene (e.g. Great White Field) reservoir. The cell count of the geocellular model is 26x26x58, which is an upscaled model to improve the run time efficiency and represents a 5000 ft x 5000 ft x 300 ft bulk volume as shown in Figure 2. The left side of Figure 2 shows the depth of the grid cells in TVDSS and the inclining structure of the reservoir. One producing well and one injection well are included in the base model with bottom hole depths of 24,900 and 25,900 ft TVDSS, respectively. Initial oil saturation is shown in the right side of Figure 2.

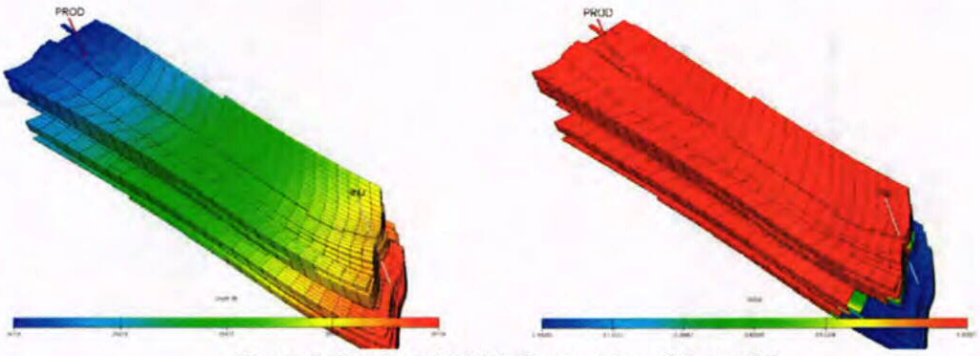

Figure 2. Depth and initial oil saturation of the model

In this study, the base case is considered as the central point case which incorporates the medium values of all static and dynamic reservoir data according to the collected reservoir data for lower tertiary reservoirs in Gulf of Mexico. The uncertainties of the reservoir parameters will be explored by assigning a high-low range to each of the parameters in the design of the experiment.

3. Uncertainty Parameters

A total of fourteen static and dynamic parameters are used in this stochastic study. The geologic uncertainty parameters incorporated into the static models include: structural dip, faulting, facies, aquifer size, and reservoir parameters (initial reservoir pressure, absolute permeability and heterogeneity). Dynamic uncertainty parameters include: fluid properties, water injection variables (timing and injection rates), and relative permeability variables (residual oil saturation and endpoints). All the uncertainty parameters are treated as independent variables as shown in Table 2. For each parameter, high and low extreme values and medium value are determined according to the extensive study on lower Tertiary reservoirs in GoM.

Table 2. Uncertainty parameters used in the design of experiment

Parameter		Real Values		
		Low	Medium	High
F1	Facies/NTG	0.5	0.8	1
F2	Formation Dip (Degree)	10	30	60
F3	Permeability (mD)	20	200	1200
F4	Aquifer Size (x HCPV)	1	5	25
F5	Fault Multiplier	0.3	0.7	1
F6	PVT/GOR (Scf/Stb)	300	1100	1800
F7	Initial Pressure Pi (Psi)	10000	15000	20000
F8	Perm Heterogeneity	0.27	0.6	0.8
F9	Sor	0.15	0.25	0.35
F10	Krw @ Sor	0.2	0.4	0.6
F11	kv/kh	0.01	0.1	1
F12	Rock Comp (10E-6 1/Psi)	1	3	10
F13	Injection Timing	0	1	3
F14	Injection Voidage	0.6	0.9	1.1

Facies Modeling

Rock facies are modeled by the Net-to-Gross (NtG) distribution by means of geostatistical methods. The base case has an average NtG of 0.8 based on the development experiences on deepwater of GoM reservoirs which consist of interbedded sheet sand and shale layers. More shales are assumed in the low case facies (left side of Figure 3) model resulting in an average NtG of 0.5. Massive clean sands are considered in the high case (right side of Figure 3). Only one porosity distribution is used in all the models, so the initial pore volume of the reservoir is determined by the NtG distribution. Since this study is focused on the incremental oil recovery by waterflooding, the depth of the OWC may not be a key factor and is not included as an uncertainty parameter. Assigning a fixed OWC depth at 21,903 ft, TVDSS, the low, base and high facies models have net initial hydrocarbon pore volume of 83.7, 104.9, and 141.7 MMRB, respectively.

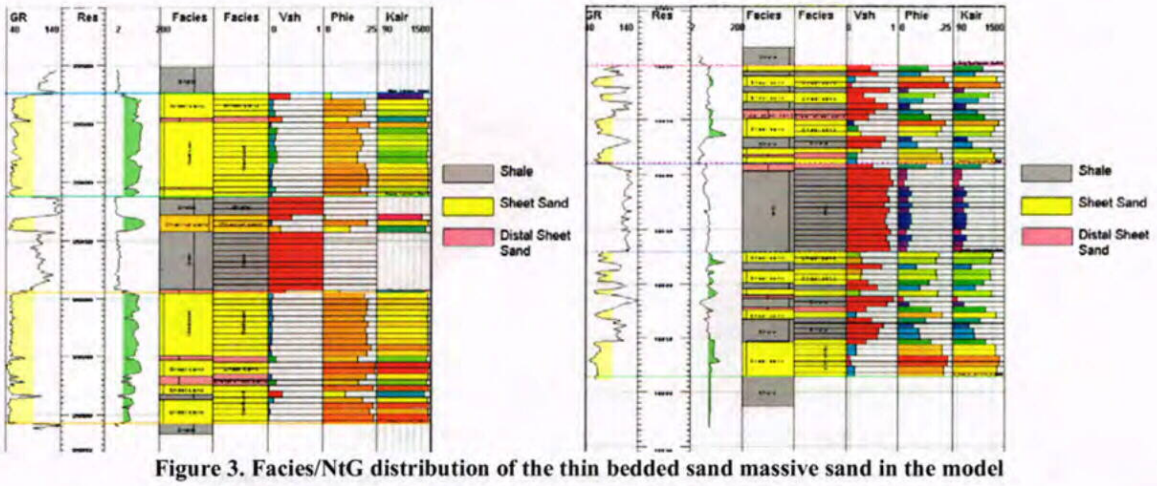

Figure 3. Facies/NtG distribution of the thin bedded sand massive sand in the model

Formation Dip

The reservoirs are inclined due to underlying salt movement, diapiric piercement or horizontal compression. The hydrocarbon migrated into an inclined geologic trap which is uplifted due to salt movement. Variations in structural dip can affect oil-water flow in the reservoir due to gravity effects. Therefore the formation dip angle is considered as an uncertainty parameter in this study with a range from 10° to 60°. Three grid systems were generated with different inclinations.

Permeability, Anisotropy and Heterogeneity

The observed permeability is typically in two distinct groups. The middle and lower Miocene reservoirs in the Green Canyon and Mississippi Canyon areas (e.g. Mad Dog and Thunder Horse) often exhibit permeability greater than 500 mD. The older Eocene and Paleocene Tertiary reservoirs often exhibit permeability less than 30 mD. In this study, the base case has an average permeability of 200md. The high and low cases of permeability cover a range from several md to 1,200 md. The results of DOE indicate that the final recovery factor is sensitive to the average permeability of the field. Reservoir anisotropy and heterogeneity are also considered as uncertainty parameters in this study.

The reservoir permeability anisotropy is represented by the ratio of vertical to horizontal permeability (Kv/Kh). A low case ratio as Kv/Kh = 0.01 is used to reflect the presence of a significant amount of thin bedded shales or a low NtG reservoir which highly restricts vertical flow. A high Kv/Kh = 1.0 is selected to represent a massive, high NtG reservoir. The medium case uses a ratio of 0.1.

Dykstra-Parsons coefficient of permeability variation is a common descriptor of reservoir heterogeneity. It measures reservoir uniformity by the dispersion or scatter of permeability values. A homogeneous reservoir has a permeability variation that approaches zero, while an extremely heterogeneous reservoir would have a permeability variation approaching one. Dykstra-Parsons coefficient of permeability can be calculated using following equation:

$$V = (K[50] - K[84])/K[50] \quad \ldots\ldots (1)$$

where $K[50]$ and $K[84]$ are permeability values corresponding to P50 and P84 percentile level. The three permeability models used in this study have Dykstra-Parsons coefficients of 0.27, 0.6 and 0.8, respectively, as shown in Figure 4.

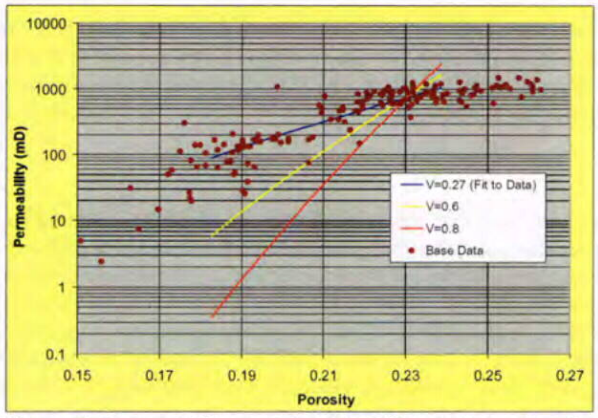

Figure 4. Permeability models with different heterogeneity

Faulting

The proxy model includes a fault, without displacement, between the updip producer and the downdip region. The transmissibility across the fault is controlled to act as a flow barrier which will reduce the drainage area and totally or partially block the communication between the producing wells and injection wells or aquifers. The base case assumes some reduction of transmissibility (multiplier of 0.7) between the updip production well area and the aquifer/injector well.

Aquifer Size

Based on the observed reservoir performance of deepwater GoM fields in water depths between 1,000 and 4,000 ft, aquifer influx is an important drive mechanism. For this study a base case aquifer to hydrocarbon pore volume (HCPV) of 5.0 times has been selected base on the performance of Pleistocene and Pliocene reservoirs. The possible sizes of the aquifer in this model are set to 1.0, 5.0 and 25 times of HCPV for low, medium and high cases, respectively.

Rock Compaction

Most of the upper Tertiary reservoirs are unconsolidated and present very high pore volume compaction like Genesis Field (40 Micro sips)[5,6,7]. The lower Tertiary reservoirs in GoM like Tahiti are typically well consolidated due to the reservoir age and depth and exhibit much lower rock compressibility and permeability reduction. In this study, the rock compressibility is assumed to be 1 to 10 $\times 10^{-6}$ psi^{-1} (Micro sips).

Initial Reservoir Pressure

Reservoirs in the deepwater GoM are unique in being over-pressured with gradients ranging from 0.60 – 0.85 psi/ft. A typical example is Thunder Horse Field where the initial reservoir pressure is approximately 16,000 psi at a subsea depth of 25,000 feet. Initial pressures in the Tahiti Field are approximately 19,000 psi. The high initial pressures will impact drive energy, water influx, and the need/timing of water injection. It is also important that oil saturation pressures typically are low (often below 5,000 psi).

Sufficient initial pressure data for the lower Tertiary reservoirs have been collected as shown in Table 1. The initial pore pressure of these reservoirs generally falls into a range from 10,000 to 20,000 psi. Fields located at the sea-ward (south) of the salt thrusts have lower reservoir pore pressures because they face the open, deep Gulf of Mexico basin. Minibasin fields, located both above salt and confined by salt, have higher pressures because they are confined and do not access an extensive basinal aquifer section. In this work, 10,000 psi and 20,000 psi are selected as the low and high case for the design of experiment, respectively.

Relative Permeability Curves

Relative permeability curves can have a big impact on reservoir flow. These curves are characterized by the curvature and end points. For waterflooding cases, it is assumed that the residual oil saturation and water relative permeability at residual oil saturation are more important to the final recovery than other curve factors. The assumed ranges of 0.15 to 0.35 for residual oil saturation and 0.2 to 0.6 for maximum water relative permeability (as shown in Table 2) cover the low and high scenarios based on the deepwater GoM development practice. The curves are derived from "Corey-type" functions and end point scaling is used in the simulation model. A capillary pressure curve that defines a small transition zone is used in the model based on observations from deepwater GoM reservoirs, like Tahiti[8].

PVT Characteristics

Extensive studies have been conducted to model the fluid properties in deepwater GoM reservoirs[9]. Fluid PVT characteristics include solution gas-oil ratio, bubble point pressure, formation volume factor and viscosity which are highly correlated to each other. In this study the PVT properties are generated with fluid characterization software particularly reflecting the correlations for GoM reservoir fluids. The solution gas-oil ratio is selected as the representative factor for the three sets of PVT data.

Injection Well Dynamics

In a design of experiment for reservoir simulation, all the parameters involved in the simulation can be sorted as uncontrollable parameters (or uncertainty parameters) and controllable parameters (or decisions)[8,10]. In theory the uncertainty parameters should only include the natural reservoir characterizations such as geological structure, rock properties and fluid properties etc. These parameters are independent to human decisions. The controllable parameters usually include number and location of wells, recovery process, artificial lift method, well configuration and control, well pattern and spacing and facility capacity etc. In a regular DOE process, only the uncontrollable parameters are used to build the deterministic P10, P50, and P90 base models. In this study small changes are made to this routine because of the nature of the problem.

The primary objective of this work is to estimate the incremental oil recovery for waterflooding given the uncertainty in other key reservoir properties. The economic benefits have not been considered; only incremental recovery factor is evaluated. Since the model is built to reflect the draining area of a single well, the injection well dynamics (injection timing and injection voidage) are the most relevant controllable parameters which affect the incremental recovery by waterflooding. Therefore, the water injection timing and injection voidage are used as uncertainty parameters. For injection timing, injection well starts simultaneously with production well in the high-side case, and three years later in the low-side case. The injection voidage is set to 0.6, 0.9, and 1.1 times as the production voidage in low, medium and high-side cases, respectively.

Design of Experiment

1. Methodology of DOE

Quantifying the uncertainty in reservoir development using design of experiment has been a steadily growing industry wide practice since the early 1990's[11,12,13,14]. As an alternative to traditional sensitivity analysis, the basic idea behind this methodology is to vary multiple parameters at the same time and explore the maximum inference with minimum time cost.

DOE is a methodology that reduces the number of reservoir simulation runs needed to generate the proxy equations (or response surface). DOE specifies a series of experiments (simulation models). The results of the simulation models can be analyzed by fitting them to a response surface, usually in the form of an analytical function or a simple numerical equation which is used as a proxy of the simulation model. Therefore a DOE study poses two main issues, designing a parameter space (experiment matrix) which covers the multiple inferences as much as possible, and generating the response surface. Yeten et al.[15] compared various methods for generating experiment design matrices and constructing response surfaces.

Experiment Designs

Full factorial design is a common method with all input factors set at two levels each[16]. These levels are marked as the high and low-side cases and represented by "-1" and "+1", respectively in the experiment matrix in this presented work. The experiment matrix contains all possible high and low combinations. Even if the number of factors N in a design is small, the 2^N runs specified by a full factorial design could be very large. For example, if 10 factors are selected in the design, there will be $2^{10} = 1024$ runs according to a two level full factorial design. In a probabilistic reservoir simulation study, it is very common to have more than 10 factors to quantify the uncertainty which makes this type of design not practical. One solution to this problem is to use only a fraction of the runs specified by the full factorial design which is called Fractional Factorial design ($2^{(N-P)}$ or $3^{(N-P)}$ design, where P is a screening number).

Plackett-Burman (PB) design and Box-Behnken (BB) design are based on the fractional factorial design. Plackett-Burman designs are very economical two-level designs where the number of runs is a multiple of four rather than a power of 2. It is known to be a very efficient screening design when only main effects are of interests. The results of a PB design can be regressed into a linear polynomial which shows the significance magnitude of each factor to the final output of the model. Box-Behnken design is a screening design of level 3. Though BB design is not as efficient as PB design, the results of a Box-Behnken design can be regressed into either a linear or a quadratic polynomial and is also efficient when the number of the factors is low.

A central composite (CC) design contains an imbedded factorial or fractional factorial design with center points that is augmented with a group of "star points" that allow estimation of curvature. The distance from the center of the design space to a star point ($|\alpha|$) is greater or equal to the distance from the center of the space to each factor. The star points equivalently extend the design space which is spanned by factors. A central composite design always contains twice as many star points as there are factors in the design.

Yeten et al. also compared some complex experiment design methods in their work such as D-Optimal (DO) design and space filling (SF) design. The order of the underlying regression model is quadratic and a more accurate response surface can be regressed using CC, DO and SP designs than using simple factorial or PB designs, but may not be sufficiently efficient in reservoir practice when the total number of factors is greater than 10. According to Yeten et al, the central composite design yields the best performance in response surface construction and uncertainty evaluation.

In this study, it is not feasible to apply central composite method for the experimental matrix design since there are 14 factors involved in the uncertainty evaluation. In this study we used a two-round method DOE as Carreras et al.[8] applied in Tahiti Field study. Plackett-Burman method is used in the first round of DOE to identify the "heavy-hitters" which presents more important parameters to the final output (recovery factor). After the first round, fewer parameters are selected for the second round design to construct a quadratic response surface using a central composite design.

Response Surface

A response surface, usually in a form of mathematical function, is used as a surrogate model or proxy which could be a good substitute of the real system or its simulation model, especially when the evaluation from a real system is impossible or expensive to simulate. Multiple linear regression is a very common method to construct the response surface in DOE. The technique uses the least squares method or other standard statistical methods to quantify the relationship between the input variables and the output response[8,17,18]. The methods to generate a response surface include least squares, Kriging, thin plate splines and artificial neural networks (ANNs). Among these four methods the least squares and ANNs methods are not data exact which means the data points are not honored by the response surface.

In this study we used least squares method to fit the response surfaces as linear or quadratic polynomials with cross terms. Least squares method is sufficiently good to construct a mathematical function composed of simple known functions, such as polynomials, which minimize the sum of the squared residuals between the simulated and function values.

2. First Round Plackett-Burman DOE

Simulation Cases

To identify the possible incremental oil recovery brought by waterflooding, DOE is applied to two groups of runs, with and without water injection, respectively. Since water injection timing and injection voidage are not applicable for no-injection runs, there are only 12 uncertainty parameters included in the DOE for no-injection cases. The Plackett-Burman designs for no-injection cases and waterflooding cases are shown in Table 3 and Table 4, respectively. Values "-1" and "1" refer to the low and high values of the uncertainty parameter, respectively.

Table 3. Plackett-Burman design matrix for no-injection cases

Exp #	F1	F2	F3	F4	F5	F6	F7	F8	F9	F10	F11	F12
1	1	1	1	1	-1	-1	1	1	-1	1	1	-1
2	-1	1	1	-1	1	1	-1	-1	-1	-1	1	-1
3	1	-1	-1	1	1	-1	1	1	-1	-1	-1	-1
4	1	-1	1	1	-1	-1	-1	-1	1	-1	1	-1
5	1	1	-1	-1	1	1	-1	1	1	-1	-1	-1
6	-1	-1	1	-1	1	-1	1	1	1	1	-1	-1
7	-1	1	-1	1	-1	1	1	1	1	-1	-1	1
8	-1	-1	-1	-1	1	-1	1	-1	1	1	1	1
9	-1	1	1	-1	-1	-1	-1	1	-1	1	-1	1
10	1	1	-1	1	1	-1	-1	-1	1	1	-1	1
11	1	-1	1	1	1	1	-1	-1	1	1	-1	1
12	-1	-1	1	1	-1	1	1	-1	-1	-1	-1	1
13	1	-1	1	-1	1	1	1	1	-1	-1	1	1
14	1	-1	-1	-1	-1	1	-1	1	-1	1	1	1
15	-1	1	-1	1	1	1	1	-1	-1	1	1	-1
16	-1	-1	-1	-1	-1	-1	-1	-1	-1	-1	-1	-1
17	1	1	1	-1	-1	1	1	-1	1	1	-1	-1
18	1	1	-1	-1	-1	-1	1	-1	1	-1	1	1
19	-1	-1	-1	1	-1	1	-1	1	1	1	1	-1
20	-1	1	1	1	1	-1	-1	1	1	-1	1	1

Table 4. Plackett-Burman design matrix for waterflooding cases

Exp #	F1	F2	F3	F4	F5	F6	F7	F8	F9	F10	F11	F12	F13	F14
1	1	-1	1	1	1	1	-1	-1	1	1	-1	1	1	-1
2	1	1	-1	-1	-1	-1	1	-1	1	-1	1	1	1	1
3	1	-1	1	1	-1	-1	-1	-1	1	-1	1	-1	1	1
4	1	-1	-1	-1	-1	1	-1	1	-1	1	1	1	1	-1
5	-1	-1	1	1	-1	1	1	-1	-1	-1	-1	1	-1	1
6	1	1	-1	-1	1	1	-1	1	1	-1	-1	-1	-1	1
7	-1	1	1	-1	-1	-1	-1	1	-1	1	-1	1	1	1
8	-1	1	-1	1	1	1	1	-1	-1	1	1	-1	1	1
9	1	1	1	-1	-1	1	1	-1	1	1	-1	-1	-1	-1
10	1	1	-1	1	1	-1	-1	-1	-1	1	-1	1	-1	1
11	1	1	1	1	-1	-1	1	1	-1	1	1	-1	-1	-1
12	-1	1	-1	1	-1	1	1	1	1	-1	-1	1	1	-1
13	1	-1	-1	1	1	-1	1	1	-1	-1	-1	-1	1	-1
14	-1	-1	1	-1	1	-1	1	1	1	1	-1	-1	1	1
15	-1	-1	-1	1	-1	1	-1	1	1	1	1	-1	-1	1
16	-1	1	1	-1	1	1	-1	-1	-1	-1	1	-1	1	-1
17	1	-1	1	-1	1	1	1	1	-1	-1	1	1	-1	1
18	-1	-1	-1	-1	-1	-1	-1	-1	-1	-1	-1	-1	-1	-1
19	-1	1	1	1	1	-1	-1	1	1	-1	1	1	-1	-1
20	-1	-1	-1	-1	1	-1	1	-1	1	1	1	1	-1	-1

Response Surfaces

The recovery factor is selected as the response variable for both no-injection and waterflooding cases. Multiple linear regressions are conducted to generate response surfaces for both group of cases in linear polynomial as shown by Equation 2 (for no-injection) and 3 (for waterflooding). For each of the cases, the response surfaces for five year recovery factor and ten year recovery factor are generated to compare the effects of parameters on short term and long term production. Plots of proxy predicted RF vs. simulation RF are plotted in Figure 5 and Figure 6 for the no-injection and waterflooding cases, respectively.

$$RF = b_0 + b_1F_1 + b_2F_2 + b_3F_3 + b_4F_4 + b_5F_5 + b_6F_6 + b_7F_7 + b_8F_8 + b_9F_9 + b_{10}F_{10} + b_{11}F_{11} + b_{12}F_{12} \quad \text{..... (2)}$$

$$RF = b_0 + b_1F_1 + b_2F_2 + b_3F_3 + b_4F_4 + b_5F_5 + b_6F_6 + b_7F_7 + b_8F_8 + b_9F_9 + b_{10}F_{10} + b_{11}F_{11} + b_{12}F_{12} + b_{13}F_{13} + b_{14}F_{14} \quad \text{..... (3)}$$

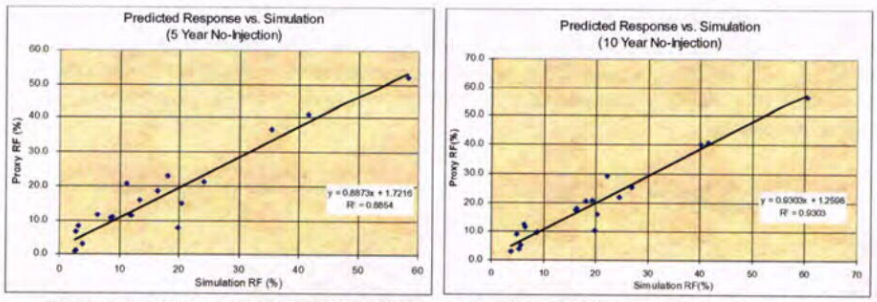

Figure 5. Plot of proxy predicted RF vs. simulation RF for no-injection cases

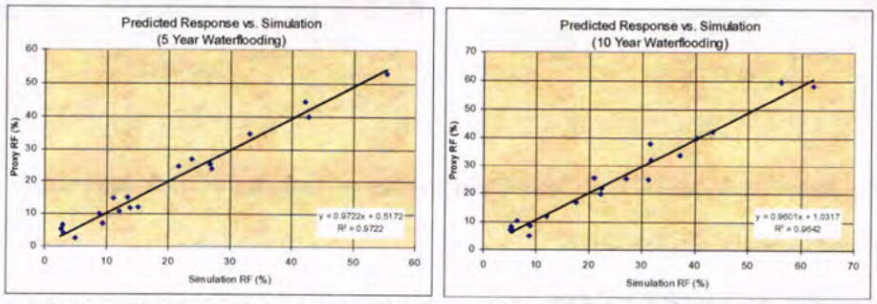

Figure 6. Plot of proxy predicted RF vs. simulation RF for waterflooding cases

Figure 5 and Figure 6, suggest that the response surfaces generated for the no-injection cases has a larger grouping of oil recovery factors at the low end. The response surfaces have captured the general trend of the simulation model and they are analyzed to identify the heavy-hitters in next step.

Heavy-Hitters for No-Injection Cases

A Pareto chart is generated using a least squares procedure for each case containing the significance values of each uncertainty parameter to the response variable (recovery factor after five or ten years production) in a descending order as shown in Figure 7. This chart is similar to the tornado chart showing the effects of each parameter on the recovery factor.

Figure 7 shows the normalized significance values for the uncertainty parameters. The contrast of the significance values is fairly big. A significance limit (blue dash line) is set on the 95% confidence level. It is noticed that both five year and ten year production cases have the same heavy-hitters. However, the permeability is more important for five year recovery. This is reasonable since the permeability value determines the initial productivity of the well and therefore the plateau rate during the first couple of years.

According to the significance limit, six uncertainty parameters are selected as the important parameters including aquifer size, permeability, PVT, formation dip, rock compaction, and initial reservoir pressure. These six parameters are used in the second round central composite design for no-injection cases.

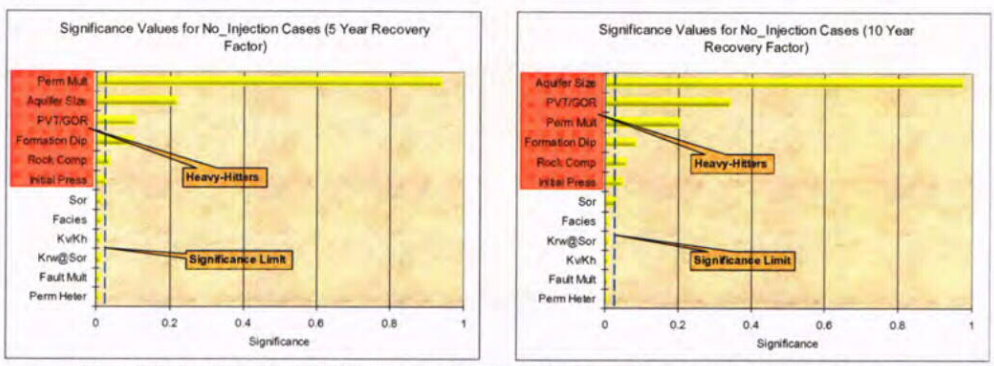

Figure 7. Pareto chart of first round Plackett-Burman design for no-injection cases

Heavy-Hitters for Waterflooding Cases

A similar analysis procedure is conducted for the waterflooding cases. The Pareto charts of the normalized significance values are plotted in Figure 8. The six heavy-hitters for the no-injection cases still present high significance for the waterflooding cases. In addition, injection timing and water relative permeability end point also affect the recovery factor with high significance. Therefore, totally eight uncertainty parameters are selected for the second round central composite design for the waterflooding cases.

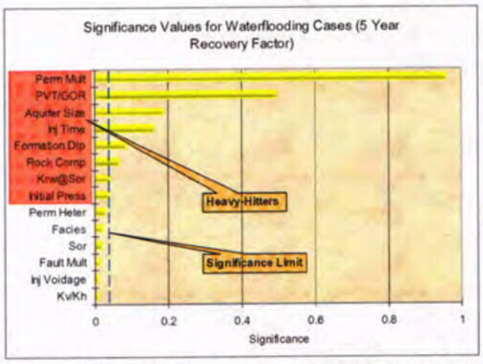

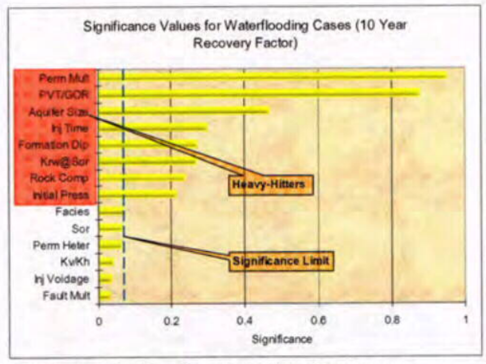

Figure 8. Pareto chart of first round Plackett-Burman design for waterflooding cases

3. Second Round Central Composite DOE

Central Composite DOE for No-Injection Cases

In the second round design, only the reduced uncertainty parameter set containing six parameters is used in the central composite DOE analysis. The experiment matrix is generated using the reduced parameter set which includes 48 cases as shown in Table 5. "-1", "0", and "1" refer to the low, medium, and high values of the parameters, respectively. Four central points are introduced in the experiment case matrix.

The central composite DOE method captures the non-linear effects and interactions on the response variable when the uncertainty parameters increase from low to high values. Based on there results of the total 48 CC experiment runs, quadratic response surfaces (polynomial) including the cross terms are generated using least squares method for five year and ten year recovery factors as represented by Equation 4.

$$RF = b_0 + b_1F_1 + b_2F_2 + ... + b_6F_6 + b_7F^2{}_1 + b_8F_1F_2 + ... + b_{12}F_1F_6 + ... + b_nF_6^2 \quad \text{.. (4)}$$

Figure 9 shows plots of the predicted recovery factors using the proxy (response surface) against the simulated recovery factors for both five and ten year production cases.

Table 5. Central composite design matrix for no-injection cases

Exp #	F1	F2	F3	F4	F5	F6	Exp #	F1	F2	F3	F4	F5	F6
1	-1	-1	1	-1	-1	1	25	0	1	0	0	0	0
2	0	0	0	0	0	0	26	1	1	-1	1	-1	1
3	-1	1	-1	1	1	1	27	0	0	-1	0	0	0
4	-1	-1	-1	-1	1	1	28	-1	1	1	-1	1	1
5	1	-1	1	1	1	-1	29	1	1	1	-1	1	-1
6	-1	1	1	1	1	-1	30	-1	1	-1	-1	-1	1
7	0	0	0	0	0	0	31	0	0	0	0	0	0
8	-1	-1	1	1	1	1	32	1	-1	-1	-1	1	-1
9	0	0	0	1	0	0	33	1	-1	1	1	-1	1
10	-1	-1	-1	1	-1	1	34	-1	1	-1	1	-1	-1
11	1	1	-1	-1	-1	-1	35	-1	0	0	0	0	0
12	1	-1	-1	1	1	1	36	1	-1	1	-1	-1	-1
13	-1	-1	1	1	-1	-1	37	0	-1	0	0	0	0
14	0	0	1	0	0	0	38	0	0	0	0	0	1
15	-1	-1	1	-1	1	-1	39	1	1	1	1	1	1
16	-1	-1	-1	-1	-1	-1	40	-1	-1	-1	1	1	-1
17	0	0	0	0	0	-1	41	-1	1	1	-1	-1	-1
18	0	0	0	-1	0	0	42	1	-1	-1	-1	-1	1
19	1	1	-1	-1	1	1	43	1	1	1	-1	-1	1
20	1	-1	-1	1	-1	-1	44	0	0	0	0	0	0
21	0	0	0	0	1	0	45	1	0	0	0	0	0
22	1	1	1	1	-1	-1	46	-1	1	-1	-1	1	-1
23	1	-1	1	-1	1	1	47	0	0	0	0	-1	0
24	1	1	-1	1	1	-1	48	-1	1	1	1	-1	1

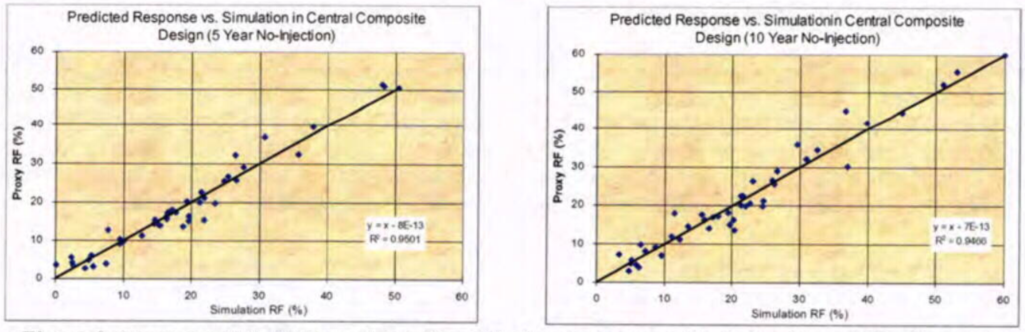

Figure 9. Proxy predicted RF vs. simulation RF of central composite design for no-injection cases

Central Composite DOE for Waterflooding Cases

In the Plackett-Burman design, eight uncertainty parameters are selected for the second round central composite design. A much largger experiment case matrix (Table 6) is generated for the waterflooding cases which consists of 88 cases including 4 central points. Similarly, based on the results of all CC design cases, a quadratic response surface is regressed in the form of Equation 5.

$$RF = b_0 + b_1F_1 + b_2F_2 + ... + b_8F_8 + b_9F^2{}_1 + b_{10}F_1F_2 + ... + b_{16}F_1F_8 + ... + b_nF_8^2 \quad \text{...} (5)$$

Table 6. Central composite design matrix for waterflooding cases

EXP#	F1	F2	F3	F4	F5	F6	F7	F8
1	1	1	-1	1	-1	-1	-1	1
2	-1	-1	-1	-1	-1	-1	1	1
3	-1	-1	1	1	-1	1	1	-1
4	1	-1	-1	-1	1	-1	-1	1
5	0	0	0	0	0	0	0	-1
6	1	-1	-1	-1	-1	1	-1	1
7	-1	1	1	1	1	1	-1	-1
8	0	0	0	0	0	1	0	0
9	-1	-1	-1	-1	1	-1	1	-1
10	1	-1	1	1	-1	1	-1	1
11	0	0	0	0	0	0	-1	0
12	1	1	1	-1	1	1	-1	1
13	-1	1	1	1	-1	1	-1	1
14	0	0	0	0	0	0	0	0
15	0	0	1	0	0	0	0	0
16	0	-1	0	0	0	0	0	0
17	0	0	0	0	0	0	0	0
18	-1	0	0	0	0	0	0	0
19	1	1	1	-1	1	-1	-1	-1
20	-1	1	1	1	1	-1	-1	1
21	1	1	-1	-1	1	1	1	1
22	0	0	0	0	0	0	0	0
23	-1	1	-1	-1	1	-1	-1	1
24	0	0	0	0	0	0	0	0
25	-1	-1	1	1	-1	-1	1	1
26	1	1	-1	-1	1	-1	1	-1
27	0	0	-1	0	0	0	0	0
28	1	1	1	1	-1	-1	1	1
29	1	-1	1	-1	1	1	1	-1
30	-1	-1	-1	-1	-1	1	1	-1

EXP#	F1	F2	F3	F4	F5	F6	F7	F8
31	1	-1	1	-1	-1	-1	1	-1
32	0	0	0	0	0	0	0	0
33	1	1	1	1	-1	1	1	-1
34	-1	-1	1	-1	-1	1	-1	-1
35	-1	-1	1	1	1	1	1	1
36	-1	-1	-1	1	-1	1	-1	-1
37	1	1	-1	1	-1	1	-1	-1
38	1	1	-1	-1	-1	-1	1	1
39	0	0	0	0	-1	0	0	0
40	0	0	0	1	0	0	0	0
41	1	1	-1	-1	-1	1	1	-1
42	1	-1	-1	1	1	-1	1	1
43	1	-1	-1	1	-1	1	1	1
44	-1	1	-1	1	-1	1	1	1
45	1	0	0	0	0	0	0	0
46	1	1	-1	1	1	1	-1	1
47	-1	-1	-1	1	1	1	-1	1
48	0	0	0	0	0	0	0	0
49	0	0	0	0	0	-1	0	0
50	1	-1	1	1	1	1	-1	-1
51	0	0	0	0	1	0	0	0
52	-1	1	1	-1	-1	-1	1	-1
53	0	0	0	0	0	0	0	0
54	-1	1	-1	-1	1	1	-1	-1
55	-1	1	-1	1	1	1	1	-1
56	-1	1	-1	-1	-1	-1	-1	-1
57	-1	1	-1	-1	-1	1	-1	1
58	0	1	0	0	0	0	0	0
59	-1	1	1	-1	1	-1	1	1
60	-1	-1	-1	1	-1	-1	-1	1

EXP#	F1	F2	F3	F4	F5	F6	F7	F8
61	0	0	0	0	0	0	1	0
62	0	0	0	0	0	0	0	1
63	0	0	0	0	0	0	0	0
64	-1	1	-1	1	-1	-1	1	-1
65	-1	1	1	1	-1	-1	-1	-1
66	1	-1	1	-1	1	-1	1	1
67	-1	-1	1	-1	1	1	-1	1
68	1	-1	-1	-1	1	1	-1	-1
69	-1	-1	1	1	1	-1	1	-1
70	-1	-1	1	-1	-1	-1	-1	1
71	1	-1	1	-1	-1	1	1	1
72	1	-1	1	1	-1	-1	-1	-1
73	1	-1	-1	1	-1	-1	1	-1
74	1	1	-1	1	1	-1	-1	-1
75	-1	1	1	-1	-1	1	1	1
76	-1	-1	-1	1	1	-1	-1	-1
77	1	-1	-1	-1	-1	-1	-1	-1
78	1	1	1	-1	-1	1	-1	-1
79	0	0	0	-1	0	0	0	0
80	-1	-1	-1	-1	1	1	1	1
81	-1	-1	1	-1	1	-1	-1	-1
82	1	1	1	1	1	1	1	1
83	1	-1	-1	1	1	1	1	-1
84	-1	1	-1	1	1	-1	1	1
85	1	1	1	1	1	-1	1	-1
86	-1	1	1	-1	1	1	1	-1
87	1	1	1	-1	-1	-1	-1	1
88	1	-1	1	1	1	-1	-1	1

Plots of the proxy predicted recovery factors vs. the simulated recovery factors are shown in Figure 10 for five and ten year production periods, respectively. The polynomial equations for both no-injection and waterflooding cases match the simulation results very well and are sufficient to be the proxy for the simulation model. These proxy equations are used in the Monte-Carlo simulation to identify P10, P50 and P90 values of recovery factor.

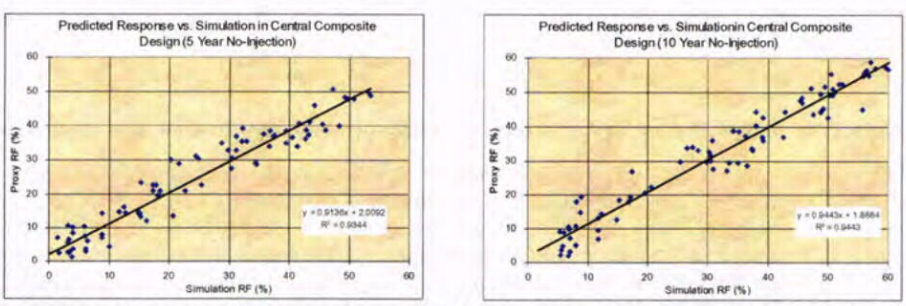

Figure 10. Proxy predicted RF vs. simulation RF of central composite design for waterflooding cases

TREX 011560.0011

4. Identify P10, P50 and P90 Values for Recovery Factor

Monte-Carlo simulations are performed to generate the probability distribution functions (PDFs). In Monte-Carlo simulation the response surface equations from CC experiment design are used to sample. Since the proxy equations are all regressed using the normalized values for each uncertainty parameter, the same type of continuous probability distribution function (normal distribution) is assigned to each parameter, with a mean equal to the medium value of the parameter and a variance of 0.2. A total of half million Monte Carlo simulations are run for both the no-injection and waterflooding cases. Some unrealistic values which count only an extreme minority of the total sampled values have been neglected.

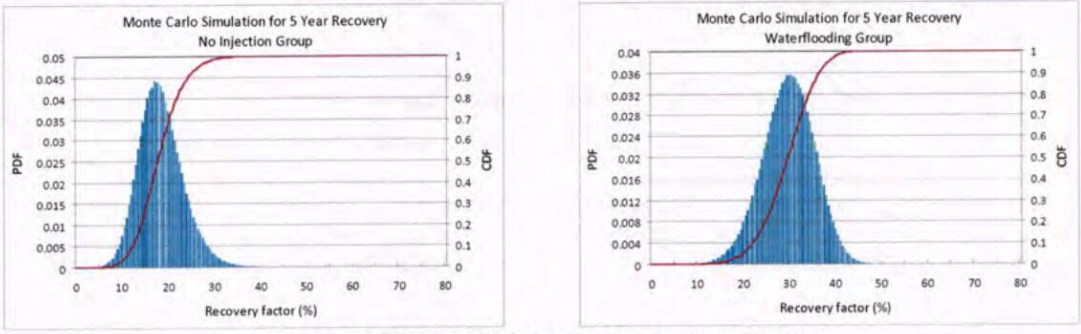

Figure 11. PDF and CDF for five year recovery factor

Comparisons of the PDF and cumulative distribution function (CDF) of five and 10 year recovery factor for both cases are shown in Figure 11 and Figure 12.

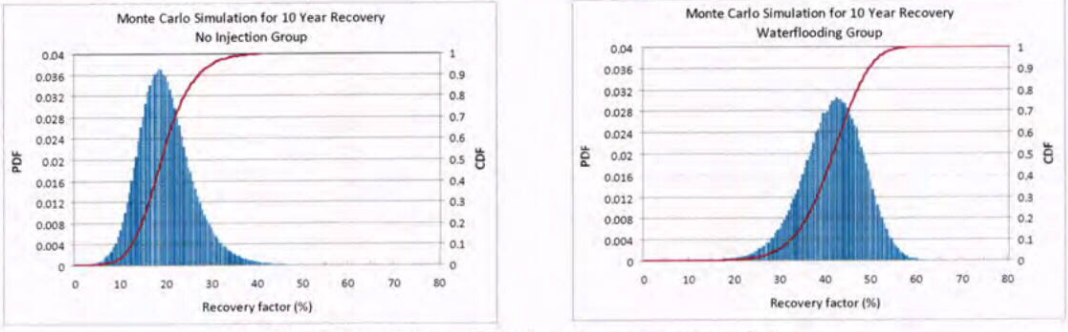

Figure 12. PDF and CDF for ten year recovery factor

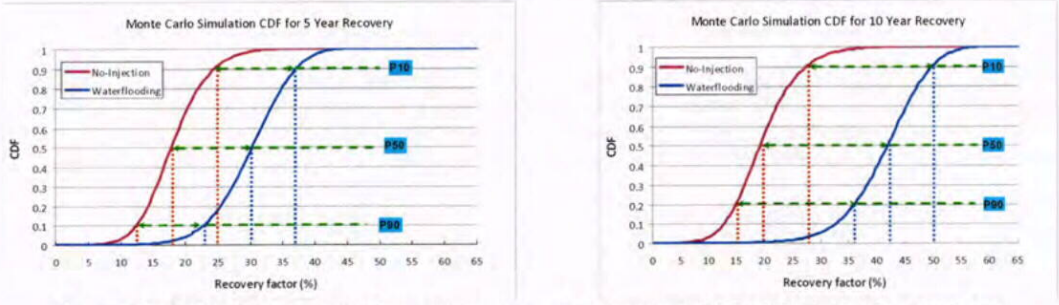

Figure 13. CDF of five year and ten year recovery factor generated by Monte-Carlo simulation

The P10, P50 and P90 recovery factors for both no-injection and waterflooding cases can be observed on Figure 13. For five year recovery case, the incremental oil recovery brought by waterflooding is around 12% of OOIP. A larger benefit, as high as 20% of OOIP incremental recovery, is expected for a ten year run according to the results of this study. Because the lower Tertiary reservoirs of deepwater GoM are usually of low permeability, low rock compaction and low solution gas-oil ratio, the driving energy of these reservoirs could be too low to maintain a long production period and achieve a high recovery factor without waterflooding. This supports the assumption proposed at the beginning of this work that waterflooding could be helpful to achieve a high final recovery in a lower Tertiary GoM reservoir.

Conclusions

1. Extensive research on the deepwater reservoir data for lower Tertiary Gulf of Mexico reservoirs was conducted through public data sources. These reservoirs are featured with deep burial, high pressure/high temperature, some with low permeability, low rock compaction, and low solution gas-oil ratio and saturation pressure.
2. Designs of experiment simulation were used to estimate the incremental oil recovery potential for water injection given the uncertainty of key reservoir parameters. With the assistance of design of experiment technique, the most important parameters can be identified and a proper proxy model can be built based on limited number of simulation runs using the reduced parameter set.
3. The results of this study indicated that those parameters with close relationships with reservoir drive energy, such as fluid properties, aquifer size, rock compaction and initial reservoir pressure, are of more significance to the recovery factor of the lower Tertiary Gulf of Mexico reservoirs. Injection timing and water relative permeability have significant impact on the recovery factor for waterflooding cases.
4. Given the range of reservoir properties observed, the recovery factors of P90, P50 and P10 confidence in five year production are 12%, 18% and 25% for no-injection case, respectively, comparing to 23%, 30% and 37% for waterflooding case. The incremental oil recovery based on the P50 estimation is 12% of OOIP.
5. For ten year production, the P90, P50, and P10 estimations of recovery factor are 15%, 20%, and 28%, respectively for no-injection case, and 36%, 42%, and 50% for waterflooding case. Waterflooding in lower Tertiary GoM reservoirs is expected to increase oil recovery by 20% of OOIP over primary methods in ten years.

Acknowledgments

The authors would like to thank Knowledge Reservoir LLC, Center of Reservoir Study of the University of Tulsa (TUCRS) and Graduate School of the University of Tulsa to jointly launch this special research project. Special thanks to all members who participated in this research project.

Nomenclatures

a_i, b_i = general coefficients
DOE = design of experiment
F_i = uncertainty parameters
K = permeability
Kv/Kh = vertical/horizontal permeability
N = total number of factors in factorial experiment design
P = screening number in factorial experiment design
RF = recovery factor
V = Dykstra-Parsons coefficient
α =distance of a parameter value from the center of DOE space

References

1. "ResKB Reservoir Data Base, version 2007", operated by Knowledge Reservoir LLC, Houston, TX.
2. "Gulf of Mexico Region Reservoir and Production Data (http://www.gomr.mms.gov/homepg/pubinfo/freeasci/freedesc.html)", the Minerals Management Service, 2007 release.
3. Website http://www.aapg.org/explorer/2006/
4. Website http://www.worldoil.com/magazine/magazine_contents.asp
5. Pourciau R.D., Fisk J.H., Descant F.J., and Waltman R.B.: "Completion and Well Performance Results, Genesis Field, Deepwater Gulf of Mexico", paper SPE 84415 presented at the 2003 SPE Annual Technical Conference and Exhibition, Denver, Colorado, 5-8 October.
6. Ring J.N., Bourgeois C.S., Howard J., Melillo A.J., Neal S.L., and Smith S.:"Management of Typhoon: A Subsea Deepwater Development", paper SPE 84147 presented at the 2003 SPE Annual Technical Conference and Exhibition, Denver, Colorado, 5-8 October.
7. R.M. Ostermeier: "Compaction Effects on Porosity and Permeability: Deepwater Gulf of Mexico Turbidite", Journal of Petroleum Technology, Volume 53, Number 2, pp. 68-74, February 2001.
8. P.E. Carreras, S.G. Johnson, and S.E. Turner: "Tahiti: Assessment of Uncertainty in a Deepwater Reservoir Using Design of Experiments", paper SPE 102988 presented at the 2006 SPE Annual Technical Conference and Exhibition, San Antonio, Texas, 24-27 September.
9. B. Dindoruk and P.G. Christman: "PVT Properties and Viscosity Correlations for Gulf of Mexico Oils", paper SPE 71633 published on Journal of Reservoir Evaluation & Engineering, Volume 7, Number 6, 427-437, December 2004.
10. M. Williams: "Assessing Dynamic Uncertainty Using Experimental Design", SPE Distinguished Lecturer Series, Houston, Texas 2006.

11. W.T. Peake, M. Abadah, and L. Skander: "Uncertainty Assessment Using Experimental Design: Minagish Oolite Reservoir", paper SPE 91820 presented at the 2005 Reservoir Simulation Symposium held in Houston, Texas, 31 Januray 2 February.
12. P.E. Carreras, S.E. Turner, and G.T. Wilkinson: "Tahiti:Development Strategy Assessment Using Design of Experiments and Response Surface Methods", paper SPE 100656 presented at the 2006 SPE Western Regional/AAPG Pacific Section/GSA Cordilleran Section Joint meeting held in Achorage, Alaska, 8-10 May.
13. C.Y., C. Uni, and R. Gupta: "Experimental Design in Deterministic Modelling: Assessing Significant Uncertainties', paper SPE 80537 presented at the 2003 SPE Asia Pacific Oil and Gas Conference and Exhibition, Jakarta, Indonesia, 9-11 September.
14. C.Y. Peng, R. Gupta, K. Vijayan, G.C. Smith, M.A. Rayfield, and D.R. DePledge: "Experimental Design Methodology for Quantifying UR Distribution Curve, Lessons Learnt and Still to Be learnt", paper SPE 88585 presented at the 2004 SPE Asia Pacific Oil and Gas Conference and Exhibition, Perth, Australia, 18-20 October.
15. B. Yeten, A. Castellini, B. Guyaguler, and W.H. Chen: "A Comparison Study on Experimental Design and Response Surface Methodologies", paper SPE 93347 presented at the 2005 Reservoir Simulation Symposium, Houston, Texas, 31 January-2 February.
16. "Experimental Design (Industrial DOE)" on website http://www.statsoft.com/textbook/stexdes.html#general#general, StatSoft, Inc., 2007.
17. B. Li and F. Friedmann: "A Novel Response Surface Methodology Based on 'Amplitude Factor' Analysis for Modeling Nonlinear Responses Caused by Both Reservoir and Controllable Factors", paper SPE 95283 presented at the 2005 SPE Annual Technical Conference and Exhibition held in Dallas, Texas, 9-12 October.
18. B. Li and F. Friedmann: "Novel Multiple Resolutions Design of Experiment/Response Surface Methodology for Uncertainty Analysis of Reservoir Simulation Forecasts", paper SPE 92853 presented at the 2005 SPE Reservoir Simulation Symposium held in Houston, Texas, 31 january-2 February.